Journal of Engineering Mathematics **40:** 159–178, 2001.

Flow efficiency of perforated systems – a combined analytical and numerical treatment

C. Y. CHEN and C. ATKINSON[1]
Division of Theoretical Mechanics, The University of Nottingham, Nottingham NG7 2RD, U.K.
[1]*Department of Mathematics, Imperial College, Queen's Gate, London SW7 2BZ, U.K.*

Received 14 April 1999; accepted in revised form 17 May 2000

Abstract. The effect of the spatial distribution of perforations on the flow from the reservoir to the wellbore for single phase liquid flow is studied. The reservoir is taken to be isotropic and, for most of the paper, the model used here assumes that the perforations and the wellbore are both undamaged. Thus, there is no change of permeability around the wellbore and perforations. The pressure/flow along a single perforation is studied in detail first and an integral equation is derived which can be solved numerically to give the pressure/flow everywhere along the perforation. The interaction of the perforations is considered by an approximation in which each perforation is represented by a point source of unknown strength positioned at the centre of the perforation. A simple ellipsoidal model of the perforation is also considered which provides a faster approach for evaluating the flow. The resulting flux of fluid from each perforation into the wellbore is presented numerically for the above-mentioned approximate methods and the comparison with the full numerical method is also made. For the ellipsoidal perforation, the modelling of the perforation skin effect (a mathematical treatment of pressure drops which is caused by perforation damage) is also described, but no detailed numerical results are given.

Key words: perforated completions, single phase flow, wellbores, oil drilling

1. Introduction

The complicated engineering process of drilling for oil requires first identifying a reservoir, usually by seismological methods. Once this has been done, a hole must be drilled with a depth of thousands of metres in general. It is then cased with steel casing and cemented. The cement is forced between the casing and the imperfect casing-rock interface in order to seal the formation. To complete the well, which is to produce oil from the formation to the surface, a communication path is created from the oil reservoir through the cement and casing to the well. For natural completions this is usually done by perforating the casing-cement formation using a perforating gun. This gun penetrates the casing, the cement, and the rock formation at a prescribed set of locations varying in depth and phase angle.

Ideally, the geometry of these perforations is designed to optimise the flow of oil from the reservoir to the well. It should also enhance well productivity by creating clear channels through the formation and by making reasonably uniform holes and entry points through the casing and cement.

Thus, the productivity of a perforated completion is influenced not only by the perforation geometry but also by the complex manner in which it interacts with the formation characteristics and the perforating environment. Figure 1 shows a typical well geometry of a perforated completion; the parameters that influence the well productivity are shot density, perforation depth, perforation diameter, and phase angle. In addition to the geometrical factors, a vari-

ety of formation physical characteristics such as formation type (sandstone, limestone, etc.), permeability, formation fluid, natural fractures, and shale laminations are also needed to be addressed. Another major consideration in well productivity is the perforation environment which includes the wellbore and perforation damage as well as the completion fluid which is used for perforation clean-up. Well deviation and differential pressure between the well and formation are also examples of environmental factors which interact with the others to determine the flux from the reservoir into the well. A damaged wellbore or perforation, for example, reduces the permeability of its surrounding area and thus affects the productivity of the perforated completion. For optimum design, each completion must be addressed individually with all applicable factors balanced as effectively as possible. The complex interaction makes some factors more important in one completion than in others. However, some of these factors such as geometric parameters, level or direction of differential pressure, and choice of completion fluid, are controllable. Various attempts at modelling these different factors have taken place over the years, a selection ([1–12]) are given in the references.

In this paper, we address the importance of the perforation geometry and study the effect of the spatial distribution of the perforations on the flow from the reservoir to the wellbore for single phase liquid flow. The parameters affecting this are:

(a) *Shot density*: number of perforations per foot.

(b) *Depth of perforation penetration* in to the reservoir.

(c) *Shot phasing*: angular pattern or perforation distribution.

(d) *Diameter of the perforated hole* in the casing and the reservoir.

To aid in deducing a semi-analytical description of the flow we will take advantage, wherever possible, of small parameters in the problem. For example, the diameter of the perforated hole is usually small, about one tenth of the wellbore diameter and about one tenth of the hole spacing. This means that, to a reasonable approximation, when we view a given perforation in a coordinate system centred on it, it feels the influence of the other perforations as if they were an unknown distribution of sources along their length. When solving the problem for this individual perforation interacting with the unknown distribution of sources for the other perforations, we get an equation for this particular open perforation's source distribution. Doing this for each perforation in turn should give us a system of algebraic equations for each of the source densities. In this way, it might be possible to even give a detailed analysis of an individual perforated hole with a damaged zone etc. and of individual perforations that may be closed. The case when perforations are close together can be treated by the full method, a modification of the method used here where we allow the full distribution of sources on each perforation to be unknown. A variety of numerical models simulating perforated completions have been considered in the literature. These include Harris [13] who used finite differences, Klots *et al.* [14] who used a finite element model, Locke [15] used a commercial finite element model in his study of perforated well productivity, and many others. For a more detailed literature survey on related numerical approaches and a recent treatment (see Dogulu [16]) in which a near-wellbore grid is coupled to a coarse block reservoir simulator.

The approach we take here can be considered complementary to the direct numerical treatments of the above authors. It can, in principle, be used to detect which of the given set of perforations is flowing. This is done when the analysis is used with a tool such as a spinner detecting pressure variations in the well. Also the details of the variation of the flow into the perforation along its length coupled together with a model for the transport of sand grains within a perforation, such as that of Pearson and Zazovsky [17], could help with understanding the problem of obtaining clean perforations.

2. Formulation of the problem

For isothermal flow of fluids of constant compressibility, c, the density ρ can be written as

$$\rho = \rho_0 \exp(c(p - p_0)), \tag{2.1}$$

where ρ_0 is the value of ρ at some reference pressure p_0. From the equation of continuity we have

$$\nabla \cdot (\rho \underline{u}) = -\frac{\partial}{\partial t}(\phi\rho), \tag{2.2}$$

where $\underline{u}$ is the velocity vector and ϕ is the porosity. From Darcy's law, valid for laminar flow at low Reynold's number, we can write (using the summation convention over repeated indices)

$$u_i = -\frac{k_{ij}}{\mu}\frac{\partial p}{\partial x_j}, \tag{2.3}$$

where μ is the viscosity of the fluid and k_{ij} is the permeability tensor of the formation assumed constant in the undamaged formation. In deducing (2.3) we have neglected the influence of gravity. Using (2.3) in (2.2), we obtain

$$\frac{\partial}{\partial x_i}\left(\frac{\rho k_{ij}}{c\mu}\frac{\partial p}{\partial x_j}\right) = \frac{\partial}{\partial t}(\phi\rho), \tag{2.4}$$

and using (2.1) we get

$$\frac{\partial}{\partial x_i}\left(\frac{k_{ij}}{c\mu}\frac{\partial p}{\partial x_j}\right) = \phi\frac{\partial \rho}{\partial t}, \tag{2.5}$$

where the porosity ϕ is assumed constant. Thus rewriting (2.5) as

$$\frac{\partial}{\partial x_i}\left(K_{ij}\frac{\partial \rho}{\partial x_j}\right) = \frac{\partial \rho}{\partial t}, \tag{2.6}$$

with $K_{ij} = k_{ij}/c\phi\mu$ a 'hydraulic diffusivity' tensor and recalling the relationship (2.1) for ρ in terms of p, we note that we have not assumed that the compressibility c is small. The usual *approximate* equation for the pressure (assuming c small) would be

$$\frac{\partial}{\partial x_i}\left(K_{ij}\frac{\partial p}{\partial x_j}\right) = \frac{\partial p}{\partial t}, \tag{2.7}$$

in the above notation. For the moment, there is no extra difficulty in working with the full Equation (2.6). Note that, if the flow is steady, we can set $\partial\rho/\partial t = 0 = \partial p/\partial t$ in Equation (2.6) or (2.7), and in principle, we can write the full problem of interactions amongst all the perforations as systems of simultaneous integral equations. Note, however, that any of these solution methods is complicated because of the non-axisymmetric nature of the perforation arrangement even in the situation when the damaged zones around the perforated holes are neglected. There is also the possibility here of treating non-isotropic permeability. Furthermore, in the analysis of Sections 3 and 4 to follow, the boundary conditions are pressure specified in the perforations and zero flux at the wellbore. This latter condition is $\nabla p = 0$ on the wellbore (for isotropic permeability) which is equivalent to $\nabla\rho = 0$ from (2.1) above. We will discuss (2.7) in what follows; however, the results can be applied to the situation of (2.7) and (2.1) by the elementary change of variable in (2.1).

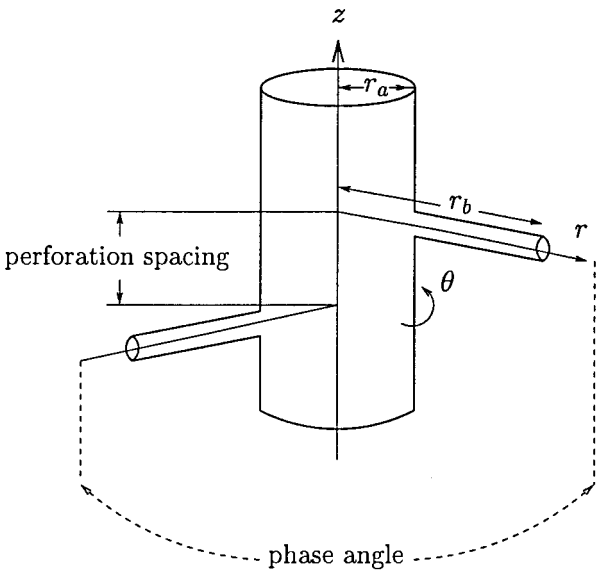

Figure 1. Wellbore geometry.

3. A single perforation

The complex interaction of the factors make it impossible to find simple global solutions to designing or analysing well completion. To further our analysis, some simplifications on formation characteristics and perforation environment are made. Thus, the analog model used here assumes

(a) ideal (undamaged) perforations,
(b) no damage around the wellbore,
(c) an isotropic reservoir.

The usual approximate equation for pressure is, from (2.7)

$$\nabla^2 p - \kappa \frac{\partial p}{\partial t} = 0, \tag{3.1}$$

where κ is the constant hydraulic diffusivity. We also assume that a constant far-field pressure has been subtracted from p so that p tends to zero at infinity. The average flux of each perforation is derived to present the effect that the spatial distribution of the perforations has on the flow. To achieve this, we first look at a single perforation in detail for the flux on the length of the perforation. The idea here is to model the flux by a continuous distribution of ring sources $Q(r)\mathrm{d}r$ of unknown strength along the perforation. We begin by considering a point source solution interacting with the wellbore boundary. This point source solution is later replaced by a ring source solution of equivalent strength. Finally, this solution is multiplied by the function $Q(r)\mathrm{d}r$ and integrated over the length of the perforation to obtain the solution required.

For convenience, a polar coordinate system (r, θ, z) is used here with the origin coinciding with the centre of the wellbore as shown in Figure 1. Assuming a point source at (r_c, θ_c, z_c) at time $t = 0$, we have the equation for pressure as,

$$\nabla^2 p - \frac{\partial p}{\partial t_1} = -\frac{\delta(r - r_c)}{r_c}\delta(\theta - \theta_c)\delta(z - z_c)\delta(t_1), \tag{3.2}$$

where $t = t_1\kappa$ has been used to absorb the hydraulic diffusivity into the time coordinate. We first take the Laplace transform over t_1 to give

$$\nabla^2 \bar{p} - s\bar{p} = -\frac{\delta(r - r_c)}{r_c}\delta(\theta - \theta_c)\delta(z - z_c). \tag{3.3}$$

Note that a source originating at a different time can easily be accommodated by multiplying the right-hand side of (3.3) by an appropriate function of s. It is further assumed that $\bar{p}$ is an even function and has Fourier series

$$\bar{p} = \frac{1}{2}\bar{p}_0(r, z) + \sum_{n=1}^{\infty} \bar{p}_n(r, z)\cos(n(\theta - \theta_c)). \tag{3.4}$$

In addition, $\delta(\theta - \theta_c)$ has Fourier series

$$\delta(\theta - \theta_c) = \frac{1}{2\pi} + \frac{1}{\pi}\sum_{n=1}^{\infty} \cos(n(\theta - \theta_c)). \tag{3.5}$$

This is substituted in Equation (3.3) and by equating the coefficients of $\cos(n(\theta - \theta_c))$, we obtain

$$\frac{1}{r}\frac{\partial}{\partial r}\left(r\frac{\partial \bar{p}_n}{\partial r}\right) + \frac{\partial^2 \bar{p}_n}{\partial z^2} - \left(s + \frac{n^2}{r^2}\right)\bar{p}_n = -\frac{1}{\pi r}\delta(r - r_c)\delta(z - z_c). \tag{3.6}$$

Taking the Fourier transform of the equation over z, the equation becomes,

$$\frac{1}{r}\frac{\partial}{\partial r}\left(r\frac{\partial \bar{\bar{p}}_n}{\partial n}\right) - \left(\zeta^2 + s + \frac{n^2}{r^2}\right)\bar{\bar{p}}_n = -\frac{1}{\pi r}\delta(r - r_c)\mathrm{e}^{\mathrm{i}\xi z_c}, \tag{3.7}$$

with

$$\bar{\bar{p}}_n = \int_{-\infty}^{\infty} \bar{p}_n \mathrm{e}^{\mathrm{i}\xi z}\,\mathrm{d}z. \tag{3.8}$$

In addition, the pressure inside the wellbore remains constant while in the reservoir, some distance away from the wellbore, the pressure is taken to be zero. Thus,

$$\left.\begin{array}{ll} \bar{\bar{p}}_n \to 0 & \text{as } r \to \infty \\ \partial\bar{\bar{p}}/\partial r = 0 & \text{on } r = r_a \end{array}\right\}, \tag{3.9}$$

where r_a is the radius of the wellbore. Equation (3.7) with the right hand side replaced by zero, satisfying the boundary condition of $\bar{\bar{p}}_n$ in Equation (3.9), has a general solution

$$\bar{\bar{p}}_n = AK_n(r\sqrt{\xi^2 + s}), \tag{3.10}$$

where K_n is a modified Bessel function of the second kind and A unknown. A particular integral is derived by substitution of $K_n(r\sqrt{\xi^2 + s})V$ in (3.7) to give

$$V = \frac{K_n(r_c\sqrt{\xi^2 + s})}{\pi}\int_{r_a}^{r} \frac{\mathrm{e}^{\mathrm{i}\xi z_c}\mathrm{d}r^*}{r^* K_n^2(r^*\sqrt{\xi^2 + s})}, \quad r_c \geq r, \tag{3.11}$$

$$= \frac{K_n(r_c\sqrt{\xi^2 + s})}{\pi}\int_{r_a}^{r_c} \frac{\mathrm{e}^{\mathrm{i}\xi z_c}\mathrm{d}r^*}{r^* K_n^2(r^*\sqrt{\xi 2^+ s})}, \quad r_c \leq r. \tag{3.12}$$

Using the boundary condition (3.9), the unknown constant A is found to be

$$A = \frac{-K_n(r_c\sqrt{\xi^2+s})\mathrm{e}^{\mathrm{i}\xi z_c}}{\pi r_a\sqrt{\xi^2+s}K_n'(r_a\sqrt{\xi^2+s})K_n(r_a\sqrt{\xi^2+s})}. \tag{3.13}$$

Thus a solution for $\bar{\bar{p}}_n$ in Equation (3.7) is

$$\bar{\bar{p}}_n = (A+V)K_n(r\sqrt{\xi^2+s}), \tag{3.14}$$

with A and V given above.

To replace the point source by a ring source in the solution, we first subtract a free-space point source solution from that above. The free-space point source solution of Equation (3.2) in the transformed domain is

$$\bar{\bar{p}}_n = V_0K_n(r\sqrt{\xi^2+s}), \tag{3.15}$$

and

$$V_0 = \frac{K_n(r_c\sqrt{\xi^2+s})}{\pi}\int_0^r \frac{\mathrm{e}^{\mathrm{i}\xi z_c}\mathrm{d}r^*}{r^*K_n^2(r^*\sqrt{\xi^2+s})}, \quad r_c \geq r, \tag{3.16}$$

$$= \frac{K_n(r_c\sqrt{\xi^2+s})}{\pi}\int_0^{r_c} \frac{\mathrm{e}^{\mathrm{i}\xi z_c}\mathrm{d}r^*}{r^*K_n^2(r^*\sqrt{\xi^2+s})}, \quad r_c \leq r. \tag{3.17}$$

Subtracting V_0 from V, we obtain

$$\begin{aligned} V - V_0 &= -\frac{K_n(r_c\sqrt{\xi^2+s})}{\pi}\int_0^{r_a} \frac{\mathrm{e}^{\mathrm{i}\xi z_c}\mathrm{d}r^*}{r^*K_n^2(r^*\sqrt{\xi^2+s})}, \\ &= -\frac{K_n(r_c\sqrt{\xi^2+s})}{\pi}\cdot\frac{I_n(r_a\sqrt{\xi^2+s})}{K_n(r_a\sqrt{\xi^2+s})}\mathrm{e}^{\mathrm{i}\xi z_c}, \end{aligned} \tag{3.18}$$

and thus,

$$\begin{aligned} A + V - V_0 &= -\frac{K_n(r_c\sqrt{\xi^2+s})}{\pi}\left(\frac{I_n(r_a\sqrt{\xi^2+s}) + r_a\sqrt{\xi^2+s}\,I_{n+1}(r_a\sqrt{\xi^2+s})}{K_n(r_a\sqrt{\xi^2+s}) - r_a\sqrt{\xi^2+s}\,K_{n+1}(r_a\sqrt{\xi^2+s})}\right)\mathrm{e}^{\mathrm{i}\xi z_c}, \\ &= -\frac{K_n(r_c\sqrt{\xi^2+s})}{\pi}\frac{I_n'(r_a\sqrt{\xi^2+s})}{K_n'(r_a\sqrt{\xi^2+s})}\mathrm{e}^{\mathrm{i}\xi z_c}. \end{aligned} \tag{3.19}$$

In Equation (3.18) above, we have used Wronskians relation (Abramowitz and Stegun [18, Equations 9.6.15 and 9.6.26] for Bessel functions, namely,

$$W\{K_\nu(z), I_\nu(z)\} = I_\nu(z)K_{\nu+1}(z) + I_{\nu+1}(z)K_\nu(z) = \frac{1}{z}, \tag{3.20}$$

and the recurrence relations,

$$\mathcal{L}_\nu'(z) = \mathcal{L}_{\nu+1}(z) + \frac{\nu}{z}\mathcal{L}_\nu(z), \tag{3.21}$$

where $\mathcal{L}_\nu(z)$ can be $I_\nu(z)$ or $\mathrm{e}^{\nu\pi\mathrm{i}}K_\nu(z)$. These relations together give, after some algebra,

$$\frac{\mathrm{d}}{\mathrm{d}z}\left(\frac{I_n(z)}{K_n(z)}\right) = \frac{1}{zK_n^2(z)}. \tag{3.22}$$

Note that $p \to 0$ as $r \to \infty$ and p is finite for $r = 0$. Taking the inverse Fourier transform of $\bar{\bar{p}}_n$ in Equation (3.14) with the point source of Equation (3.15) removed, the solution, denoted by $\bar{p}_w$, is

$$\begin{aligned}\bar{p}_w &= \frac{-1}{2\pi^2}\int_0^\infty K_0(r\tilde{\xi})K_0(r_c\tilde{\xi})\frac{I_0'(r_a\tilde{\xi})}{K_0'(r_a\tilde{\xi})}\cos(\xi(z-z_c))\mathrm{d}\xi,\\ &-\frac{1}{\pi^2}\sum_{n=1}^{\infty}\cos(n(\theta-\theta_c))\int_0^\infty K_n(r\tilde{\xi})K_n(r_c\tilde{\xi})\frac{I_n'(r_a\tilde{\xi})}{K_n'(r_a\tilde{\xi})}\cos(\xi(z-z_c))\mathrm{d}\xi,\end{aligned} \tag{3.23}$$

and $\tilde{\xi} = \sqrt{\xi^2+s}$. Note that if we make the approximation that the wellbore radius r_a is much less than r_c, a simple approximation to $\bar{p}_w$ can be deduced. (See Equation (A.13) in the Appendix.)

For the ring source solution required, we take the point source solution for $\nabla^2\bar{p} - s\bar{p} = 0$ and integrate over the ring. Thus, denoting the solution by $\bar{p}_r$, we have

$$\begin{aligned}\bar{p}_r &= \frac{1}{4\pi}\int_0^{2\pi}\frac{\mathrm{e}^{-\sqrt{s}R}\rho\mathrm{d}\phi}{R}\\ &= \frac{1}{4\pi}\int_0^{2\pi}\frac{\rho\mathrm{d}\phi}{R} + \frac{1}{4\pi}\int_0^{2\pi}\frac{(\mathrm{e}^{-\sqrt{s}R}-1)}{R}\rho\mathrm{d}\phi,\end{aligned} \tag{3.24}$$

where ρ, not to be confused with the density used earlier, is the radius of the ring and $R = \sqrt{(x-x_c)^2+(y-y_c)^2+(z-z_c)^2}$ where (x_c, y_c, z_c) are the coordinates of the point source on the ring. Note that we have assumed that the centre of the ring coincides with the x-axis and thus the coordinates on the ring can be written as $(x_c, \rho\cos\phi, \rho\sin\phi)$. By changing the integration variable from $\phi = \phi_1 - \pi$ and using the substitution $\cos\phi_1 = 1 - 2\sin^2(\phi_1/2)$, we may write Equation (3.24) as follows

$$\bar{p}_r = \frac{\rho}{\pi}\frac{k(m_c)}{\sqrt{(\sqrt{y^2+z^2}+\rho)^2+(x-x_c)^2}} + \frac{\rho}{\pi}\frac{\overline{k}(m_c)}{((\sqrt{y^2+z^2}+\rho)^2+(x-x_c)^2}, \tag{3.25}$$

where $k(m_c)$ is the complete elliptic integral of the first kind (Abramowitz and Stengun [18, Equation 17.3.1]). Both $k(m_c)$ and $\overline{k}(m_c)$ depend on y, z, ρ and $x - x_c$ with

$$k(m_c) = \int_0^{\pi/2}\frac{\mathrm{d}\phi}{\sqrt{1-m_c\sin^2\phi}}, \quad m_c = \frac{4\rho\sqrt{y^2+z^2}}{(\sqrt{y^2+z^2}+\rho)^2+(x-x_c)^2}, \tag{3.26}$$

and

$$\bar{k}(m_c) = \int_0^{\pi/2}\frac{\mathrm{e}^{\sqrt{s}\sqrt{1-m_c\sin^2\phi}\sqrt{(\sqrt{y^2+z^2}+\rho)^2+(x-x_c)^2}}-1}{\sqrt{1-m_c\sin^2\phi}}\mathrm{d}\phi. \tag{3.27}$$

Note that when $y^2 + z^2 = \rho^2$ and $x = x_c$, i.e. $m_c = 1$, $k(m_c)$ diverges at $\pi/2$ while $\overline{k}(m_c)$ remains finite. The elliptic function $k(m_c)$ has a limit

$$\lim_{m_c \to 1} k(m_c) \to \frac{1}{2} \log \left(\frac{16}{1 - m_c} \right). \tag{3.28}$$

Thus, writing

$$k_0(m_c) = k(m_c) - \frac{1}{2} \log \left(\frac{16}{1 - m_c} \right), \tag{3.29}$$

we may remove the singularity and obtain

$$\log \left(\frac{16}{1 - m_c} \right) = \log(16(4\rho^2 + (x - x_c)^2) - 2 \log |x - x_c|. \tag{3.30}$$

The only singularity is when $x = x_c$ for the term $\log |x - x_c|$, which can be dealt with separately without too much complication.

As described at the beginning of the section, we can now combine the three solutions together. This is done by taking the point source solution with the wellbore boundary, subtracting out the point source solution of an infinite medium and replacing it with a ring source solution. Superposing over the length of the perforation, the solutions $\bar{p}_r$ and $\bar{p}_w$ are multiplied by some unknown density function $Q(r)\mathrm{d}r$ along the perforation to give,

$$\bar{p}(r, \theta, z) = \frac{1}{2\pi} \int_{r_a}^{r_b} Q(r_c) \bar{p}_r(r, \theta, z) \mathrm{d}r_c + \int_{r_a}^{r_b} Q(r_c) \bar{p}_w(r, \theta, z) \, \mathrm{d}r_c, \tag{3.31}$$

where r_a is the radius of the wellbore and r_b is the end of the perforation. The two solutions $\bar{p}_r$ and $\bar{p}_w$ are also functions of r_c, θ_c, and z_c. Note that the density function $Q(r_c)$ in the first integral is divided by 2π to ensure that the point source is of equal strength to that of the ring source solution in the limit $\rho \to 0$. It is also assumed that, within the perforations, the pressure remains constant. Thus, for $y^2 + z^2 = \rho^2$ and $\theta = \theta_c$, $p = p_f$, a constant. This condition could, of course, be easily generalised by replacing the constant p_f with a function of r on the perforation. The unknown density function in Equation (3.31) can be evaluated numerically by discretising the integrals into n intervals over r and r_c to give a system of $n + 1$ equations with $n + 1$ unknowns, namely $Q(r_i)$'s, $i = 1, 2, \ldots n + 1$. The system is inverted numerically to give $Q(r_i)$'s along the perforation.

Note also the function $Q(r)$ could be singular at both ends of the integral. To avoid this, a simple change of integration variable is required, i.e.

$$r_c = \left(\frac{r_a - r_b}{2} \right) (1 - \cos \phi) + r_b,$$

$$r = \left(\frac{r_a - r_b}{2} \right) (1 - \cos \theta_0) + r_b, \tag{3.33}$$

and

$$Q(r_c) = \frac{F(\phi)}{\sin \phi}. \tag{3.34}$$

The formulation given here applies to the full transient problem. In principle, the time dependence of the pore pressure profile in the formulation could be determined by solving (3.31) for discrete values of s, the Laplace transform variable, and inverting the Laplace transform numerically. However, detailed results will be given for the steady state case, $s \to 0$, of the above formation.

Some simple limiting results can be obtained from the full formulation (3.31). Multiplying (3.24) by $1/s$ and inverting the Laplace transforms, we obtain

$$p_r = \frac{1}{4\pi}\int_0^{2\pi}\frac{\rho}{R}\mathrm{d}\phi + \frac{1}{4\pi}\int_0^{2\pi}\left(\mathrm{erfc}\left(\frac{R}{2\sqrt{t_1}}\right)-1\right)\frac{\rho}{R}\mathrm{d}\phi. \tag{3.35}$$

The first term leads to the steady state limit used in the next section. If we expand the second term as t_1 tends to infinity, we get

$$p_r = \frac{1}{4\pi}\int_0^{2\pi}\frac{\rho}{R}\mathrm{d}\phi + \frac{1}{4\pi^{3/2}}\frac{1}{t_1^{1/2}}\int_0^{2\pi}\rho\mathrm{d}\phi + O(t_1^{-3/2}). \tag{3.36}$$

Thus it can be seen that as t_1 tends to infinity, Equation (3.31) tends to the steady-state equations with a correction term tending to zero like $\rho\bar{Q}/(t^{1/2}4\pi^{3/2})$, where $t = t_1\kappa$, κ being the hydraulic diffusivity in (3.1) and

$$\bar{Q} = \int_{r_a}^{r_b} Q(r_c)\mathrm{d}r_c. \tag{3.37}$$

4. Interaction between perforations

The first example considered below is that of a steady state flow. As a consequence, the Laplace transform variable s is dropped from the equations above and the overbar of p is ignored. The interaction between the perforations is characterised by the resulting average density function $Q(r)$'s of the perforations. It is expected that each perforation is at some distance away from the others so that the effect one perforation has on the others can be approximated by $\bar{Q}\cdot\bar{H}(r,\theta,z)$ at the centre of the perforation. Evaluated at $r_c = (r_a + r_b)/2$, the functions are given by

$$\bar{Q}_i = \int_{r_a}^{r_b} Q_i(r_c)\mathrm{d}r_c, \tag{4.1}$$

and

$$\bar{H}_j(r,\theta,z) = \left(\frac{1}{4\pi R} + p_w(r,\theta,z)\right)_{r_c=(r_a+r_b)/2}, \tag{4.2}$$

where $R = \sqrt{(x-x_c)^2+(y-y_c)^2+(z-z_c)^2}$ with (x_c, y_c, z_c) being the centre of the perforation. In this case, each perforation is seen by all the others as if it were a source (or sink) of unknown strength, denoted by $\bar{Q}$, acting at the centre of the perforation and interacting with the impermeable wellbore. Thus, for the interaction of all N perforations together, the following equation is obtained,

$$p(r,\theta,z) = \int_{r_a}^{r_b} H_j(r,\theta,z)\,Q_j(r_c)\mathrm{d}r_c + \sum_{i=1,i\neq j}^{N}\bar{Q}_j\bar{H}_j(r,\theta,z)_{r_c=(r_a+r_b)/2}, \tag{4.3}$$

where the subscripts i and j relate the functions to the corresponding perforations for $j = 1, 2, \ldots, N$. Note that $H_j(r,\theta,z)$ is different from $\bar{H}_i(r,\theta,z)$ and defined as

$$H_j(r,\theta,z) = \left(\frac{1}{2\pi}p_r(r,\theta,z) + p_w(r,\theta,z)\right)_{r_c=(r_a+r_b)/2}, \tag{4.4}$$

with $\bar{p}_w$ and $\bar{p}_r$ given by Equations (3.23) and (3.24) ignoring the Laplace transform variable. Thus, on the boundary of perforation j where $z = z_j, \theta = \theta_j$, and $r_a < r < r_b$, we have

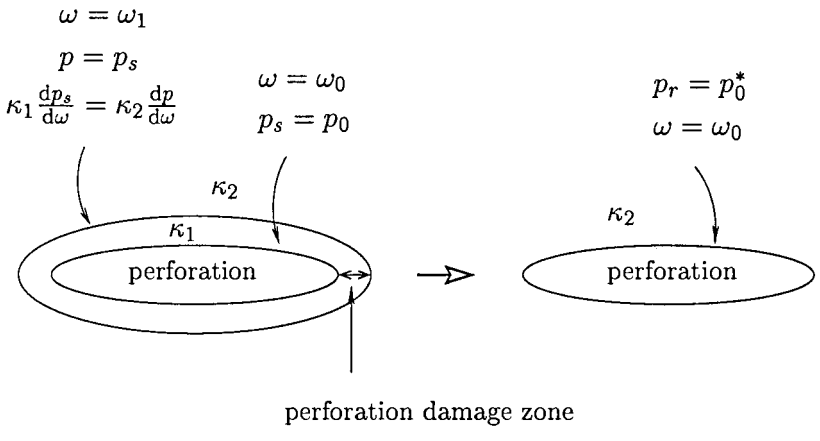

Figure 2. The skin effect

$$p_f = \int_{r_a}^{r_b} H_j(r, \theta_j, z_j) Q_j(r_c)\, \mathrm{d}r_c + \sum_{i=1, i\neq j}^{N} \bar{Q}_i \bar{H}_i(r, \theta_j, z_j)_{r_c=(r_a+r_b)/2}, \tag{4.5}$$

where $\bar{Q}_i$'s are unknowns and p_f is a constant. Discretising both r and r_c into n intervals, denoted by r_s and r_t respectively with the subscripts $s, t = 1, 2, \ldots n$, we obtain the following system of equations,

$$\underline{p}_f(s) = A(s,t)\underline{Q}_j(t) + \sum_{i=1, i\neq j}^{N} \bar{Q}_i \underline{\bar{H}}_i(s), \tag{4.6}$$

where matrix $A(s,t)$ corresponds to $H_j(r, \theta_j, z_j)$ evaluated at $r = r_s$ and $r_c = r_t$. Similarly, vectors $\underline{Q}_j(t)$ and $\underline{H}_i(s)$ correspond to functions Q_j and H_i at $r = r_s$ and $r_c = r_t$ while $\underline{p}_f(s)$ is a constant vector. Writing Equation (4.6) as

$$A^{-1}(t,s)\underline{p}_f(s) = \underline{Q}_j(t) + \sum_{i=1, i\neq j}^{N} \bar{Q}_i A^{-1}(t,s)\underline{\bar{H}}_i(s), \tag{4.7}$$

we can integrate over r_c from r_a to r_b to give

$$\int_{r_a}^{r_b} A^{-1}(t,s)\underline{p}_f(s)\mathrm{d}r_c = \bar{Q}_j + \sum_{i=1, i\neq j}^{N} \bar{Q}_i \int_{r_a}^{r_b} A^{-1}(t,s)\underline{\bar{H}}_i(s)\mathrm{d}r_c. \tag{4.8}$$

This procedure gives a system of N equations for $j = 1, 2, \ldots N$ with N unknown $\bar{Q}_j$'s. The solution for this gives the N average $\bar{Q}_j$'s.

5. Perforation skin effect

For the results obtained so far, we have assumed ideal perforations. This means that no perforation damage has occurred during well completion. However, the same procedure can still be used when the perforation is surrounded by a damaged zone. In this case, the skin effect due to the perforation damage is absorbed into the boundary condition. In what follows, a brief description of modelling this skin effect is given.

The perforation is assumed to take the shape of an ellipsoid with the permeability of the skin, the damage zone, being $\kappa = \kappa_1$, and $\kappa = \kappa_2$ as the formation permeability (see Figure 2). Isotropy is assumed in both regions. To model the skin effect on the perforation with a prescribed boundary condition, we derive another system with a modified constant pressure on the perforation boundary. However, the fluxes into the perforations of both models must remain the same. Using the substitution

$$\frac{x^2}{\omega + a_1} + \frac{y^2}{\omega + a_2} + \frac{z^2}{\omega + a_3} = 1, \tag{5.1}$$

and assuming that p depends only on ω, we observe that the equation $\nabla^2 p = 0$ becomes

$$\frac{\mathrm{d}^2 p}{\mathrm{d}\omega^2} + \frac{1}{2}\left(\frac{1}{\omega + a_1} + \frac{1}{\omega + a_2} + \frac{1}{\omega + a_3}\right)\frac{\mathrm{d}p}{\mathrm{d}\omega} = 0. \tag{5.2}$$

A treatment of certain nonlinear diffusion models using a somewhat similar approach can be found in Atkinson [19]. On the boundary of the perforation $\omega = \omega_0$, the pressure remains constant. Assuming the region of the damaged zone is bounded by $\omega = \omega_0$ and $\omega = \omega_1$, we expect the pressure to be continuous across the boundary. In addition, the flux is also continuous across the perforation boundary $\omega = \omega_1$. Thus, the boundary conditions are

$$p_s = p, \quad \text{on} \quad \omega = \omega_0, \tag{5.3}$$

and

$$p = p_s, \quad \kappa_1 \frac{\mathrm{d}p_s}{\mathrm{d}\omega} = \kappa_2 \frac{\mathrm{d}p}{\mathrm{d}\omega} \quad \text{on} \quad \omega = \omega_1, \tag{5.4}$$

where p and p_s denote the pressure distribution in the reservoir and skin, respectively. Integrating Equation (5.2), we have

$$\frac{\mathrm{d}p}{\mathrm{d}\omega} = \frac{A_2}{\sqrt{(\omega + a_1)(\omega + a_2)(\omega + a_3)}}. \tag{5.5}$$

Subject to the continuity of pressure across the boundary, Equation (5.5) is integrated further to give the pressure in the reservoir as

$$p = \frac{A_2}{\sqrt{a_1 - a_2}} \log \left| \frac{\sqrt{\omega + a_1} - \sqrt{a_1 - a_2}}{\sqrt{\omega + a_1} + \sqrt{a_2 - a_2}} \right|, \tag{5.6}$$

with $a_2 = a_3$, $a_1 > a_2$ and A_2 unknown, whereas the pressure in the damage zone is found to be

$$\begin{aligned} p_s = {} & \frac{A_1}{\sqrt{a_1 - a_2}} \left\{ \log \left| \frac{\sqrt{\omega + a_1} - \sqrt{a_1 - a_2}}{\sqrt{\omega + a_1} + \sqrt{a_1 - a_2}} \right| - \log \left| \frac{\sqrt{\omega_1 + a_1} - \sqrt{a_1 - a_2}}{\sqrt{\omega_1 + a_1} + \sqrt{a_1 - a_2}} \right| \right\} \\ & + \frac{A_2}{\sqrt{a_1 - a_2}} \log \left| \frac{\sqrt{\omega + a_1} - \sqrt{a_1 - a_2}}{\sqrt{\omega + a_1} + \sqrt{a_1 - a_2}} \right|. \end{aligned} \tag{5.7}$$

Continuity of flux on the perforation boundary $\omega = \omega_1$ requires

$$\kappa_1 \frac{\mathrm{d}p_s}{\mathrm{d}\omega} = \kappa_2 \frac{\mathrm{d}p}{\mathrm{d}\omega}. \tag{5.8}$$

This gives $A_2(\kappa_2 - \kappa_1) = \kappa_1 A_1 \mathrm{l}$. Finally, using the boundary condition $p = p_0$ at $\omega = \omega_0$, we derive

$$p_0 = \frac{A_1}{\sqrt{a_1 - a_2}} \left\{ \left(\frac{\kappa_2}{\kappa_2 - \kappa_1} \right) \log \left| \frac{\sqrt{\omega_0 + a_1} - \sqrt{a_1 - a_2}}{\sqrt{\omega_0 + a_1} + \sqrt{a_1 - a_2}} \right| - \log \left| \frac{\sqrt{\omega_1 + a_1} - \sqrt{a_1 - a_2}}{\sqrt{\omega_1 + a_1} + \sqrt{a_1 - a_2}} \right| \right\}. \tag{5.9}$$

The flux produced by this skin model at the perforation boundary is

$$\kappa_1 \frac{\mathrm{d}p_s}{\mathrm{d}\omega} \quad \text{at} \quad \omega = \omega_0. \tag{5.10}$$

A second model of a homogeneous reservoir without skin but with a modified pressure boundary condition inside the perforation, *e.g.* $p_r = p_0^*$ at $\omega = \omega_0$, has solution

$$p_r = \frac{p_0^*}{\sqrt{a_1 - a_2}} \left(\log \left| \frac{\sqrt{\omega + a_1} - \sqrt{a_1 - a_2}}{\sqrt{\omega + a_1} + \sqrt{a_1 - a_2}} \right| - \log \left| \frac{\sqrt{\omega_0 + a_1} - \sqrt{a_1 - a_2}}{\sqrt{\omega_0 + a_1} + \sqrt{a_1 - a_2}} \right| \right), \tag{5.11}$$

and permeability κ_2. The fluxes into the perforation from these two models can be made the same if we chose p_0^* such that

$$\kappa_1 = \frac{\mathrm{d}p_s}{\mathrm{d}\omega} = \kappa_2 \frac{\mathrm{d}p_r}{\mathrm{d}\omega} \quad \text{at} \quad \omega = \omega_0. \tag{5.12}$$

This gives the result

$$p_0^* = \frac{p_0(\kappa_1/\kappa_2) \log \left| \dfrac{\sqrt{\omega_0 + a_1} - \sqrt{a_1 + a_2}}{\sqrt{\omega_0 + a_2} + \sqrt{a_1 - a_2}} \right|}{\log \left| \dfrac{\sqrt{\omega_0 + a_1} - \sqrt{a_1 + a_2}}{\sqrt{\omega_0 + a_2} + \sqrt{a_1 - a_2}} \right| - \left(1 - \dfrac{\kappa_1}{\kappa_2} \right) \log \left| \dfrac{\sqrt{\omega_1 + a_1} - \sqrt{a_1 + a_2}}{\sqrt{\omega_1 + a_2} + \sqrt{a_1 - a_2}} \right|}. \tag{5.13}$$

6. Approximation method

When considering the interaction between the perforations in Section 4, we assume that, from a distance, the effect of the perforation can be approximated by the average of $Q(r)$ over the length of the perforation, denoted by Q_{avg}, evaluated at the centre of the perforation. This idea is extended further in this section to derive an approximation method for the evaluation of Q_{avg}.

In order to take into account the interaction between an individual perforation and the wellbore, we imagine the wellbore sees the perforation as if it were a source or sink of unknown strength sitting at its centre. By solving for the interaction between this source and the wellbore, we are then able to distribute the resulting pressure field, which is felt back at the perforation, uniformly over the above mentioned ellipsoidal model of the perforation.

The interaction between the point and the wellbore is derived as before and the resulting pressure field, due to the point source, is given by equations (3.10)–(3.13). The point source is to be replaced by an ellipsoid. Thus, removing the point source, we have

$$\begin{aligned} p_w &= \frac{-1}{2\pi^2}\int_0^\infty K_0(r\tilde{\xi})K_0(r_c\tilde{\xi})\frac{I_0'(r_a\tilde{\xi})}{K_0'(r_a\tilde{\xi})}\cos(\xi(z-z_c))\,\mathrm{d}\xi, \\ &-\frac{1}{\pi^2}\sum_{n=1}^{\infty}\cos(n(\theta-\theta_c))\int_0^\infty K_n(r\tilde{\xi})K_n(r_c\tilde{\xi})\frac{I_n'(r_a\tilde{\xi})}{K_n'(r_a\tilde{\xi})}\cos(\xi(z-z_c))\,\mathrm{d}\xi, \end{aligned} \tag{6.1}$$

which is multiplied by some unknown Q at $r_c = (r_b + r_a)/2$. The pressure field for the ellipsoid in a homogeneous region as derived in the previous section, without the wellbore, is

$$p_e = \frac{-1}{8\pi\sqrt{a_1 - a_2}}\log\left|\frac{\sqrt{\omega + a_1} - \sqrt{a_1 - a_2}}{\sqrt{\omega + a_1} + \sqrt{a_1 - a_2}}\right|, \tag{6.2}$$

multiplied again by some unknown strength Q with $a_2 = a_3$ and $a_1 > a_2$. Note that as $R \to \infty$, $p_e \to 1/4\pi R$ which agrees with the point source at infinity. Thus, for a single perforation interacting with the wellbore, the pressure field can be approximated by

$$p(r, z, \theta; w) = \{p_w(r, z, \theta; r_c, z_c, \theta_c) + p_e(w)\}Q, \tag{6.3}$$

where

$$\frac{(x - x_e)^2}{\omega + a_1} + \frac{(y - y_e)^2}{\omega + a_2} + \frac{(z - z_e)^2}{\omega + a_3} = 1, \tag{6.4}$$

with (x_e, y_e, z_e) being the centre of the ellipsoid. For a single perforation, the unknown constant Q is solved by imposing the boundary condition that the differential pressure remains constant, p_f say, on $w = 0$.

For the interaction of the n perforations, we use the same argument as before. That is the effect of the perforation i on perforation j is approximated by a point source sitting at the centre of the ellipsoid. Thus, on the boundary of perforation j, we have

$$p_f = Q_j p_j(r_j, \theta_j, z_j; \omega_j) + \sum_{i=1; i\neq j}^{n} Q_i \tilde{p}_i(r_j, \theta_j, z_j; r_i, \theta_i, z_i), \tag{6.5}$$

with the assumption that $\omega_j = 0$ for p_j and (r_j, θ_j, z_j) is the centre of perforation ellipsoid j. Note that the approximation of perforation i by a point source is given by

$$\tilde{p}_i(r_j, \theta_j, z_j; r_i, \theta_i, z_i) = p_w(r_j, z_j, \theta_j; r_i, z_i, \theta_i) + \frac{1}{4\pi R}, \tag{6.6}$$

evaluated at $r_i = (r_a + r_b)/2$ while p_j remains as

$$p_j(r, \theta, z; w) = p_w(r, z, \theta; r_j, z_j, \theta_j) + p_e(w). \tag{6.7}$$

Equation (6.5) then gives a system of n equations which is solved numerically to give the n Q_i's.

7. Results

The flux of fluid across a control surface is defined as

$$\int_A \underline{u}.\underline{n}\,\mathrm{d}A, \tag{7.1}$$

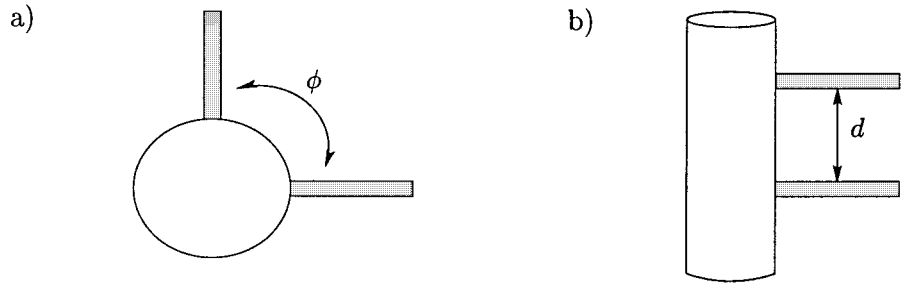

Figure 3. An example of perforation arrangements on a) the horizontal plane and b) the vertical plane.

where A is the area of surface and $\underline{n}$ is normal to the surface. From Darcy's law,

$$u_i = -\frac{\kappa_{ij}}{\mu}\frac{\partial p}{\partial x_j}, \tag{7.2}$$

with $\kappa_{ij} = \kappa\delta_{ij}$ for an isotropic medium. Thus the flow into the well from a given perforation is

$$A\left(\frac{\kappa}{\mu}\frac{\partial p}{\partial r}\right) = -\frac{\kappa}{\mu}\int_{\tau_a}^{\tau_b} Q(r)\,\mathrm{d}r. \tag{7.3}$$

Note that the flux of fluid due to the ring source or its equivalent point source is given by $\int_s (\partial p/\partial R)\,\mathrm{d}s$ and $p \to Q/(4\pi R)$ as $R \to \infty$, where s is the surface of the sphere and R is the distance from its centre. Thus the flux of the ring is found to be $-Q(\kappa/\mu)$.

The interaction between the perforations, as described in the previous sections, is simplified by the assumption that the effect of a perforation, when observing it from another perforation, can be approximated by a point source sitting at its centre. The accuracy of this assumption is verified in the table below using an example describing the interaction of two perforations.

The results discussed here are all evaluated with the typical values given below

wellbore radius	:	4 inches,
perforation radius	:	0.1 inches,
perforation length	:	10 inches,
differential pressure	:	$-p_d$ psi.

7.1. The interaction between two perforations in the same vertical plane

It is assumed that the two perforations lie on the same vertical plane $\theta = 0$ at some distance d apart. The resulting flux from each perforation into the well is thus expected to be symmetric. If the full solution outlined in Section 3, Equation (3.31), are used for a single perforation, the resulting pressure field due to the two perforations can be written as

$$p(r,\theta,z) = \int_{r_a}^{r_b} H_1(r,\theta,z)Q(r_1)\,\mathrm{d}r_1 + \int_{r_a}^{r_b} H_2(r,\theta,z)Q(r_2)\,\mathrm{d}r_2, \tag{7.4}$$

with H_1 and H_2 defined as Equation (4.4) in Section 4. The above equation is solved to give $Q(r)$ along the length of the perforation which is later integrated over the perforation to give the total flux denoted by Q_α. This result is then compared with the flux, Q_β, derived from Equation (4.5) in Section 4 where a point source approximation is assumed for the interacting perforation, *i.e.*

Table 1. The resulting flux into the well of two perforations interacting on the same vertical plane with distance d inches apart.

d	Q_α	Q_β	Q_γ
5	−10·65768	−10·58205	−10·55519
10	−11·43545	−11·41567	−11·31184
12	−11·60656	−11·59670	−11·49447
20	−11·98124	−11·99208	−11·87493

$$p(r,\theta,z) = \int_{\tau_a}^{\tau_b} H_i(r,\theta,z)\,Q_i(r_i)\,\mathrm{d}r_i + \bar{Q}_j \bar{H}_j(r,\theta,z), \tag{7.5}$$

where $i, j = 1, 2$ and $i \neq j$ with H_i given by Equation (4.4) and $\bar{H}_j$ by Equation (4.2).

The approximation method in Section 6, where the perforation is replaced by an ellipsoid, gives another comparison to the above two methods. The flux derived here will be denoted by Q_γ, by use of the equation

$$p_f = Q_j\,p_j(r_j,\theta_j,z_j;\omega_j) + \sum_{i=1;i\neq j}^{n} Q_i\,\tilde{p}_i(r_j,\theta_j,z_j;r_i,\theta_i,z_i), \tag{7.6}$$

with p_j and $\tilde{p}_i$ given by Equations (6.3) and (6.6). For this case, on the right of Equation (7.6), we set $r_j = r_a$. This means that the effect of the wellbore on the ellipsoid is felt more on those parts closer to the wellbore than far away. This approximation is not very important for the effect of perforations far away and is justified by the agreement shown in Table 1. The resulting flux of the above three methods are listed in Table 1 for various values of distance between perforations. Note that for all the results in this section, the flux Q has been scaled by the factor $p_d\kappa/\mu$.

7.2. The interaction between two perforations on the same horizontal plane

For this situation, there is also symmetry between the perforations so that Equation (6.3) applies and full solution of the integral equation gives the flux Q_α. The approximation where one perforation is replaced by a single source of unknown strength gives the flux Q_β and the ellipsoidal approximation the flux Q_γ. As can be seen in Table 2, these approximations are quite close to the full solution given by Q_α.

7.3. The interaction of n perforations symmetrically placed in the same horizontal plane

This generalises the problem of Section 7.2 above and again a comparison, given in Table 3, between the full solution flux Q_α and the approximation Q_β and Q_γ can be made.

Table 2. The resulting flux into the well of two perforations interacting on the same horizontal plane with distance ϕ apart.

ϕ	Q_α	Q_β	Q_γ
$\pi/4$	−10·99771	−10·97143	−10·60587
$\pi/2$	−11·71390	−11·70034	−11·41816
π	−12·06837	−12·05609	−11·87454

Table 3. The resulting flux into the well with n perforations evenly placed on the same horizontal plane.

n	Q_α	Q_β	Q_γ
2	−12·06837	−12·05609	−11·87454
3	−11·30102	−11·27820	−10·96279
4	−10·51301	−10·47365	−10·03359

7.4. More general perforation arrangement

We present solutions by both approximate methods for perforations separated by a vertical distance d and at various phase angles, all perforations having the same length. It can be seen from Table 4 that the ordering of the fluxes is the same for both methods though the fluxes

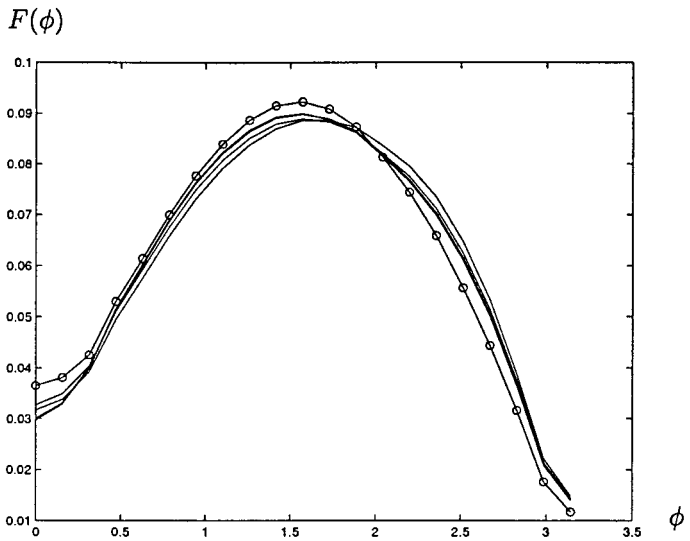

Figure 4. Variation of flux along perforations. The circled curve is that given by a single perforation interacting with the wellbore. The others are the flux variations from the example in Table 4 (Q_β case) where symmetry is expected about the centre of the wellbore and consequently only four curves are shown.

Table 4. The resulting flux into the well with perforations spiral down the well; d is the vertical separation and ϕ is the phase angle.

d	ϕ	Q_β	Q_γ
0	0	−11·2753	−10·1317
10	$\pi/4$	−10·5016	−9·6374
20	$\pi/2$	−10·1000	−9·4937
30	$3\pi/4$	−9·9527	−9·3960
40	0	−9·9527	−9·3960
50	$\pi/4$	−10·0997	−9·4937
60	$\pi/2$	−10·5017	−9·6374
70	$3\pi/4$	−11·2756	−10·1316

calculated by the simple ellipsoid method are somewhat smaller than those predicted by the method in Section 4.

7.5. Flux variation along perforations

As well as the average flux into a given perforation, the solution of the integral equation (3.31) gives the variation of this flux along the perforation itself. Results for this variation are given in Figure 4 for $F(\phi)$ of (3.34) and are presented for the cases outlined in Table 4 as well as for a single perforation. All of these examples of perforations interact with the wellbore and the resulting curves are normalised by the corresponding average flux into each perforation. Since the actual flux into each perforation is given by (3.34), *i.e.* the values in the curve divided by $\sin(\phi)$, we would expect $F(\phi)$ to tend to zero as ϕ tends to π which is the position of the wellbore in this coordinate system (see Equation (3.32)). This is indeed the case shown by the numerical results. Furthermore, the actual variations along each perforation is much the same when normalised by the average flux which is what we might expect. In addition, the actual flux is greatest at the end of the perforation in the matrix as it is singular there when we revert to coordinates in terms of r_c using (3.32).

8. Discussion

The full numerical solution of the integral equation formation (3.31) for a single perforation interacting with the wellbore gives a flux $Q_\alpha = -12{\cdot}6263$ while the approximation of representing the perforation by an ellipsoid and its interaction with the wellbore approximated by the method of Section 6 gives $Q_\gamma = -12{\cdot}5228$. Tables 1, 2, 3 and 4 can be used to show how different arrangements of perforations compete for the flow of fluid. For example, in Table 1, as the spacing between two perforations in the same vertical plane increases, the flux into each perforation increases but it is still less than that of an isolated perforation. For the situation where the perforations are spaced in a horizontal plane, Tables 2 and 3, the interaction again reduces the flux to individual perforation as might be expected. For example, in the case of two perforations, the least interaction is when the perforations are at opposite sides of the wellbore where the wellbore partially shields one from the other.

This paper has described methods which treat the problem of flow into a wellbore through perforations to various degrees of accuracy. First, the complete problem of a straight well in a formation of isotropic permeability was analysed for the full transient problem of an undamaged reservoir. The problem was reduced to integral equations along each perforation. This problem becomes computer intensive if many perforations are involved and thus for the steady flow case, certain approximations are used. The first of these replaces distant perforations by unknown source strengths when attention is directed to a particular perforation. The variable source density of this particular perforation is then used to calculated its average source strength as seen from the other perforations. This means that detailed calculation of each perforation leads to a set of simultaneous equations for the average source strengths. Finally, the flow into each perforation is compared with that from the full solution. The same strategy is also applied to a simple ellipsoidal model for each perforation. These simpler approximations thus become practicable for dealing with completion strategies which involve many perforations distributed around the wellbore. Work on extending these methods to this practical situation and allowing for anisotropic permeabilities is in progress.

Appendix. An approximate solution for p_w – For the point source field of the steady flow problem

For a point source of the strength Q at position (x_c, y_c, z_c), the field at position (r, θ, z) is given by

$$p_c = \frac{Q}{4\pi\sqrt{r^2 + r_c^2 - 2rr_c\ \cos(\theta - \theta_c) + (z - z_c)^2}}, \tag{A.1}$$

with

$$\frac{\partial p_c}{\partial r} = \frac{-Q[r - r_c\ \cos(\theta - \theta_c)]}{4\pi R^{3/2}} \tag{A.2}$$

and $R^2 = r^2 + r_c^2 - 2rr_c\ \cos(\theta - \theta_c) + (z - z_c)^2$.

If we assume that the wellbore radius r_a is much less than r_c (*i.e.* $r_a \ll r_c$) then we can approximate $\partial p_c/\partial r$ at the wellbore by

$$\left(\frac{\partial p_c}{\partial r}\right)_{r=r_a} \approx \frac{Qr_c\ \cos(\theta - \theta_c)}{4\pi R_0^{3/2}}, \tag{A.3}$$

with $R_0^2 = r_c^2 + (z - z_c)^2$.

We wish to represent the fluid pressure field p for the source together with an impermeable wellbore as

$$p = p_c + p_w. \tag{A.4}$$

Thus to evaluate p_w we need to solve $\nabla^2 p_w = 0$ with p_w tending to zero at infinity and

$$\left(\frac{\partial p_w}{\partial r}\right)_{r=r_a} \approx \frac{-Qr_c\ \cos(\theta - \theta_c)}{4\pi R_0^{3/2}}, \tag{A.5}$$

at $r = r_a$. This last condition is an approximation based on the preceding argument with $r_a \ll r_c$. It is clear of course that, whereas replacing R by R_0 should be a good approximation in this case, the approximation of the denominator is not so good when $\theta - \theta_c = \pi/2$. However, with r_a sufficiently small this should not be a major error.

Since $\nabla^2 p_w = 0$ can be written as

$$\frac{1}{r}\frac{\partial}{\partial r}\left(r\frac{\partial p_w}{\partial r}\right)+\frac{1}{r^2}\frac{\partial^2 p_w}{\partial \theta^2}+\frac{\partial^2 p_w}{\partial z^2}=0, \tag{A.6}$$

in cylindrical polar coordinates, we look for a solution in the form

$$p_w=\bar{p}_w\ \cos(\theta-\theta_c), \tag{A.7}$$

and apply a Fourier transform over z to obtain

$$\frac{1}{r}\frac{\partial}{\partial r}\left(r\frac{\partial \bar{\bar{p}}_w}{\partial r}\right)-\left(\xi^2+\frac{1}{r^2}\right)\bar{\bar{p}}_w=0, \tag{A.8}$$

where

$$\bar{\bar{p}}=\int_{-\infty}^{\infty} e^{i\xi z}\bar{p}_w\ dz. \tag{A.9}$$

The condition on $\partial p_w/\partial r$ at $r=r_a$ gives

$$\left(\frac{\partial \bar{\bar{p}}_w}{\partial r}\right)_{r=r_a}=\frac{-Q}{2\pi}\xi K_1(r_c\xi)e^{i\xi z_c}, \tag{A.10}$$

since

$$\int_{-\infty}^{\infty}\frac{e^{i\xi z'}}{(r_c^2+z'^2)^{3/2}}\,dz'=\frac{2\xi}{r_c}K_1(r_c\xi). \tag{A.11}$$

The solution of $\nabla^2 p=0$ satisfying this condition can be written as

$$\bar{\bar{p}}_w=\frac{-Q}{2\pi}\frac{K_1(r_c\xi)}{K_1'(r_a\xi)}K_1(r\xi)\ e^{i\xi z_x}, \tag{A.12}$$

where $K_1'(z)=dK_1(z)/dz$.

Inverting this transform and referring back to p_w, we have

$$p_w=\frac{-Q}{2\pi}\frac{\cos(\theta-\theta_c)}{\pi}\int_0^{\infty}\frac{\cos(\xi(z-z_c))K_1(r\xi)K_1(r_c\xi)}{K_1'(r_a\xi)}\,d\xi, \tag{A.13}$$

This result looks somewhat different from that given in Equation (3.23). It is a great deal simpler but is, of course, an approximation and should be compared with (3.23) multiplied by Q. Noting that $I_1'(z)=1/2$ as z tends to zero, whereas $\lim_{z\to 0} I_n'(z)=0$ for $n\neq 1$, we see that the above result then agrees with (3.23) if we allow the crude approximation of taking these limits inside the integral sign.

Acknowledgements

The first author would like to thank Schlumberger Cambridge Research for their financial support.

References

1. J.M. McDowell and M. Muskat, The effect on well productivity of formation penetration beyond perforated casing. *Trans. Am. Inst. Mining, Metall. Petr. Eng.* 189 (1950) 309–312.
2. A.F. Van Everdingen, The skin effect and its influence on the productive capacity of a well. *Trans. Am. Inst. Mining, Metall. Petr. Eng.* 198 (1953) 17l–176.
3. M.H. Harris, The effect of perforating on well productivity, *J. Petr. Eng.* (April 1996) 518–28.
4. K.C. Hong, Productivity of perforated completions in formations with or without damage. *J. Petr. Eng.* (Aug. 1975) 1027–1038.
5. S. Locke, An advanced methods for predicting the productivity ratio of a perforated well. *J. Petr. Eng.* (Dec. 1981) 2481–2488.
6. S.M. Tariq, M.J. Ichara and L. Ayestaran, Performance of perforated completions in the presence of anisotropy, laminations, or natural fractures. *Soc. Petr. Engrs.* (Nov. 1989) 376–884.
7. H.O. Jr. McLeod, The effect of perforating conditions on well performance. *J. Petr. Eng.* (Jan. 1983) 31–39.
8. L.A. Behrmann and T.Y. Hsia, Perforating skin as a function of rock permeability and underbalance. Paper SPE 22810 presented at the 1991 SPE Annual Technical Conference and Exhibition, Dallas, Oct. 6–9.
9. J.M. Bonomo and W.S. Young, Analysis and evaluation of perforating and perforation cleanup methods. *J. Petr. Eng.* (March 1985) 505–510.
10. E.A. Jr. Colle, Increased production with underbalance perforations. *Pet. Eng. Intl.* (July 1978) 39–42.
11. R.F. Krueger, An overview of formation damage and well productivity in oilfield operation. *J. Petr. Eng.* (Feb. 1986) 131–152.
12. J.A. Regalbuto and R.S. Riggs, Underbalanced perforation characteristics as affected by differential pressure. *Soc. Petr. Engrs.* (Feb. 1988) 83–88.
13. M.H. Harris, The effect of perforating on well productivity. *J. Petr. Eng.* (1996) 518–628.
14. J.A. Koltz, R.F. Kruger and D.S. Pye, Effect of perforation damage on well productivity. *J. Petr. Eng.* (1974) 1303–1314.
15. S. Locke, An advanced method for predicting the productivity ratio of a perforated well, *J. Petr. Eng.* (1981) 2481–2488.
16. Y.S. Dogulu, Modeling of well productivity in perforated completions. *Soc. Petr. Engrs. paper 51048*, presented at the 1998 Annual Technical Conference and Exhibition, New Orleans, Louisiana.
17. J.R.A. Pearson and A.F. Zazorsky, A model for the transport of sand grains from a perforation during underbalance surge. *Soc. Petr. Engrs. paper 38634*, presented at the 1997 Annual Technical Conference and Exhibition, San Antonio, Texas.
18. M. Abramowitz and I.A. Stegun, *Handbook of Mathematical Functions*. New York: Dover (1965) 1046 p.
19. C. Atkinson, Asymptotic methods applied to problems of diffusion, crack propagation and crack tip stress analysis, in mathematical models and methods in mechanics. Banach Center Publ. (1985) 7–48.